REPORT No. 841

APPLICATION OF THE METHOD OF CHARACTERISTICS TO SUPERSONIC ROTATIONAL FLOW

By Antonio Ferri

SUMMARY

A system for calculating the physical properties of supersonic rotational flow with axial symmetry and supersonic rotational flow in a two-dimensional field was determined by use of the characteristics method. The system was applied to the study of external and internal flow for supersonic inlets with axial symmetry. For a circular conical inlet the shock that occurred at the lip of the inlet became stronger as it approached the axis of the inlet and became a normal shock at the axis. The region in which strong shock occurred increased with the increase of the angle of internal cone at the lip of the inlet. For an inlet with a central body the method of characteristics was applied to the design of an internal-channel shape that, theoretically, results in very efficient recompression in the inlet; it was shown that if an effuser is connected with the diffuser a body of revolution with very small shock-wave drag can be determined.

INTRODUCTION

The characteristics method for the determination of supersonic phenomena was first used by Prandtl and Busemann for two-dimensional flow (references 1 and 2). For flow with axial symmetry Frankl (reference 3) used the method of characteristics for determining the shape of a supersonic circular effuser with uniform exit velocity, and Ferrari (references 4 and 5) independently used the characteristics method for determining supersonic phenomena for every type of boundary condition. Subsequently Guderley (reference 6) and Sauer (reference 7) transformed the system proposed by Frankl and Ferrari and obtained a different analytical solution of the problem. In all applications the hypothesis of potential flow was made; therefore the equation of potential flow was used.

When shock waves that are not plane (two-dimensional flow) or conical (flow with axial symmetry) occur in uniform flow, the variation of entropy across the shock is not constant and the flow behind the shock is no longer isentropic and becomes rotational. If the variation of entropy is small, the effect of rotation of the flow is not important for determining the pressure distribution along a body and the theory of potential flow gives correct results. If the shock wave is strong and has large curvature, however, the effect of the rotation becomes important and the flow must be considered as rotational.

The method of characteristics can be extended to apply to rotational flow if, in place of the potential function for the differential equation of motion, the stream function considered by Crocco (reference 8) is used. With the characteristics method for rotational flow a more exact determination can be made of the shape of the shock wave and the distribution of velocity and pressure for phenomena in which the effect of rotation is important, as in the internal flow through supersonic inlets. The procedure of numerical calculation is similar and not much more complicated than that used for the case of potential flow with axial symmetry.

SYMBOLS

p	pressure
ρ	density
s	entropy, mechanical units
V	velocity
M	Mach number
V_l	limiting velocity corresponding to adiabatic expansion to zero pressure
a	speed of sound
W	ratio of velocity to limiting velocity $\left(\frac{V}{V_l}\right)$
$c=\frac{a}{V_l}$	
u	x-component of relative velocity
v	y-component of relative velocity
x, y	Cartesian coordinates
β	Mach angle $\left(\text{arc sin } \frac{1}{M}\right)$
φ	angle between velocity V and x-axis, radians
ϵ	angle between tangent to shock and direction of velocity of flow in front of shock
δ	deviation of direction of velocity across shock wave
θ	angle of polar coordinate in conical field
ϕ	potential function
ψ	stream function for rotational flow (see equation (11))
γ	ratio of specific heat at constant pressure and constant volume
R	gas constant
n	normal to streamline

$l=\frac{\sin\beta\tan\beta\sin\varphi}{\cos(\varphi+\beta)}$

$m=\frac{\sin\beta\tan\beta\sin\varphi}{\cos(\varphi-\beta)}$

H, L, K, and N defined by equation (14)

$\xi_1=x_A-x_B$

$\xi_0=x_C-x_A$

$h=\frac{W_A}{W_B}$

$g=1+\frac{\xi_1}{\xi_0}$

$e=\frac{\sin\beta_A}{\cos(\beta_A+\varphi_A)}$

$f=\frac{\sin\beta_B}{\cos(\varphi_B-\beta_B)}$

$r=\tan\beta_A+h\tan\beta_B$

$A=\frac{s_B-s_A}{\gamma R}\,\frac{1}{e+gf}$

Subscripts:

- 0 chamber condition (zero-velocity adiabatic transformation)
- A points of first family
- B points of second family
- C quantities in the points calculated from A and B
- x derivative with respect to x
- y derivative with respect to y
- a ahead of shock
- b behind shock
- φC_n value corresponding to value of φ at point C_n
- C_n at point C_n

CHARACTERISTICS METHOD FOR SUPERSONIC POTENTIAL FLOW WITH AXIAL SYMMETRY

The differential equation for potential flow with axial symmetry (reference 4) is

$$\left(1-\frac{\phi_x^2}{a^2}\right)\frac{\partial^2\phi}{\partial x^2}+\left(1-\frac{\phi_y^2}{a^2}\right)\frac{\partial^2\phi}{\partial y^2}-\frac{2\phi_x\phi_y}{a^2}\frac{\partial^2\phi}{\partial x\partial y}+\frac{v}{y}=0 \quad (1)$$

In supersonic flow some lines can be individuated (characteristic lines) that divide the flow into two regions for which the values of ϕ, ϕ_x, and ϕ_y along the line are different. For every point of the flow two characteristic lines can be determined; every line is inclined at the Mach angle with respect to the direction of the velocity at the point, and therefore the characteristic lines can be divided into two families on the basis of the sign of the angle of the characteristic line with respect to the direction of the velocity. A family that is usually called the first family is defined by the equation

$$\frac{dy}{dx}=\tan(\beta+\varphi) \quad (2)$$

and the other family (second family) is defined by

$$\frac{dy}{dx}=\tan(\varphi-\beta) \quad (3)$$

The variation of the quantities that define the velocity (φ and V) along a characteristic line is given by the following equations from reference 5:

For the first family,

$$\frac{dV}{V}-d\varphi\tan\beta-l\frac{dx}{y}=0 \quad (4)$$

and for the second family,

$$\frac{dV}{V}+d\varphi\tan\beta-m\frac{dx}{y}=0 \quad (5)$$

where l and m are trigonometric expressions defined as

$$\left.\begin{aligned} l&=\frac{\sin\beta\sin\varphi\tan\beta}{\cos(\beta+\varphi)}\\ m&=\frac{\sin\beta\sin\varphi\tan\beta}{\cos(\varphi-\beta)}\end{aligned}\right\} \quad (6)$$

If the direction of the velocity and the Mach number at two points near each other (points A and B in fig. 1) are known, the direction of the velocity and the Mach number at a point C given by the intersection of the two characteristic lines of different family starting from points A and B can be determined. Because the distances BC and AC are small, all the coefficients of equations (4) and (5) can be considered constant and coincident to the corresponding values at points B and A, and the tangents to the characteristic lines at points A and B can be substituted for the characteristic lines from point A to point C and from point B to point C. In this case the lines AC and BC are straight lines. The line BC is inclined at an angle $\varphi-\beta$ with respect to the x-axis and the line AC is inclined at an angle $\varphi+\beta$ with

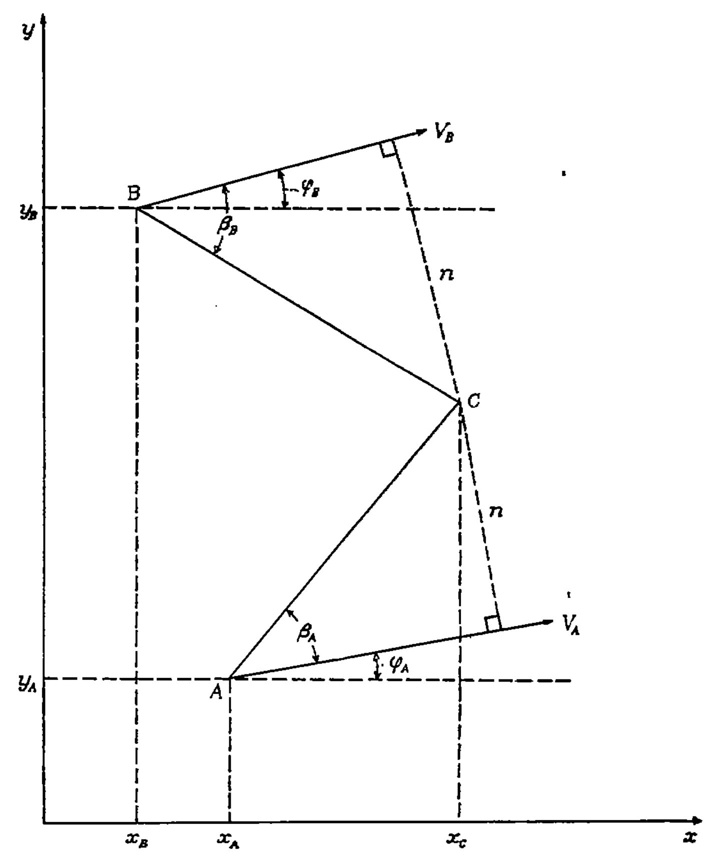

FIGURE 1.—Geometrical construction for determining point C by the characteristics method.

respect to the x-axis. Equation (4) can be applied for the line AC where

$$dx = x_C - x_A$$
$$y = y_A$$
$$V = V_A$$
$$\beta = \beta_A$$
$$l = l_A$$

and equation (5) can be applied for the line BC where

$$dx = x_C - x_B$$
$$y = y_B$$
$$V = V_B$$
$$\beta = \beta_B$$
$$m = m_B$$

For practical use equations (4) and (5) are combined and transformed by means of the ratio W of the velocity V to the limiting velocity V_l. This ratio is defined as

$$\left(\frac{V_l}{V}\right)^2 = \frac{1}{W^2} = 1 + \frac{2}{\gamma - 1}\sin^2\beta \tag{7}$$

and the following equations are obtained:

$$d\varphi_A\left(\tan\beta_B + \frac{W_A}{W_B}\tan\beta_A\right) = 1 - \frac{W_A}{W_B} - (\varphi_A - \varphi_B)\tan\beta_B + \frac{m_B}{y_B}(x_C - x_B) - (x_C - x_A)\frac{l_A}{y_A}\frac{W_A}{W_B} \tag{8}$$

$$\frac{dW_A}{W_A} = \tan\beta_A\, d\varphi_A + \frac{(x_C - x_A)l_A}{y_A} \tag{9}$$

$$\left.\begin{aligned} W_C &= W_A + dW_A \\ \varphi_C &= \varphi_A + d\varphi_A \end{aligned}\right\} \tag{10}$$

With the method of characteristics (reference 4) it can be shown that, if a deviation of a streamline which wets the body occurs, the phenomena on the corner are regulated by the same laws that regulate the two-dimensional flow; therefore, the tangents of every characteristic line starting from the corner are known. If the initial flow conditions are known, the step-by-step calculation of all the physical properties of the flow in the entire field is permitted, particularly the calculation of the shape of the shock wave and the pressure distribution along any body of revolution with axial symmetrical flow in cases in which the hypothesis of potential flow is correct.

CHARACTERISTICS METHOD FOR SUPERSONIC ROTATIONAL FLOW WITH AXIAL SYMMETRY

Supersonic perfect flow is rotational when the flow is preceded by a shock wave and when the variation of entropy across the shock wave changes from point to point behind the shock. In this case the transformation of the fluid along every streamline is isentropic until another shock wave occurs in the fluid (reference 8).

If a stream function ψ is assumed to be defined by the following equations from reference 8:

$$\left.\begin{aligned} \psi_y &= yu(1-W^2)^{\frac{1}{\gamma-1}} \\ \psi_x &= -yv(1-W^2)^{\frac{1}{\gamma-1}} \end{aligned}\right\} \tag{11}$$

the equation

$$f(\psi) = \frac{v_x - u_y}{y(1-W^2)^{\frac{\gamma}{\gamma-1}}} \tag{12}$$

is a function of only the stream function ψ (reference 8); and therefore from the equations of state, continuity, energy, and steady motion the following equation can be obtained:

$$\left(1 - \frac{u^2}{c^2}\right)\psi_{xx} - \frac{2uv}{c^2}\psi_{xy} + \left(1 - \frac{v^2}{c^2}\right)\psi_{yy} - \frac{\psi_y}{y} - y^2(1-W^2)^{\frac{\gamma+1}{\gamma-1}}\left(\frac{W^2}{c^2} - 1\right)f(\psi) = 0 \tag{13}$$

Equation (13) is a Monge-Ampère equation, and if

$$H = 1 - \frac{u^2}{c^2}$$

$$L = 1 - \frac{v^2}{c^2}$$

$$K = -\frac{uv}{c^2}$$

$$N = -\frac{\psi_y}{y} - y^2(1-W^2)^{\frac{\gamma+1}{\gamma-1}}\left(\frac{W^2}{c^2} - 1\right)f(\psi) \tag{14}$$

two characteristic families with the following equations can be obtained: For the first family,

$$\frac{dy}{dx} = \frac{K}{H} - \sqrt{\frac{K^2}{H^2} - \frac{L}{H}} \tag{15}$$

$$\psi_{xx} + \left(\frac{K}{H} + \sqrt{\frac{K^2}{H^2} - \frac{L}{H}}\right)\psi_{yx} + \frac{N}{H} = 0 \tag{16}$$

and for the second family,

$$\frac{dy}{dx} = \frac{K}{H} + \sqrt{\frac{K^2}{H^2} - \frac{L}{H}} \tag{17}$$

$$\psi_{xx} + \left(\frac{K}{H} - \sqrt{\frac{K^2}{H^2} - \frac{L}{H}}\right)\psi_{yx} + \frac{N}{H} = 0 \tag{18}$$

If n is the normal to the streamline, equation (11) yields

$$\psi_x^2 + \psi_y^2 = y^2W^2(1-W^2)^{\frac{2}{\gamma-1}} = \left(\frac{d\psi}{dn}\right)^2 = \text{grad}^2\psi \tag{19}$$

and

$$\frac{\text{curl }\mathbf{V}\times\mathbf{V}}{a^2} = \frac{1}{\gamma R}\text{grad } s = \frac{1}{\gamma R}\frac{ds}{dn} \tag{20}$$

because s is constant along every streamline; therefore

$$f(\psi) = \frac{\gamma - 1}{2\gamma}\frac{1}{R}\frac{ds}{dn}\frac{1}{yW(1-W^2)^{\frac{1}{\gamma-1}}} \tag{21}$$

and the following expressions can be obtained:

$$\left.\begin{aligned}\psi_{xx}&=-yv_x(1-W^2)^{\frac{1}{\gamma-1}}-\frac{dy}{dx}(1-W^2)^{\frac{1}{\gamma-1}}v\\&\quad+\frac{2yvW}{\gamma-1}(1-W^2)^{\frac{-\gamma+2}{\gamma-1}}W_x\\\psi_{yx}&=yu_x(1-W^2)^{\frac{1}{\gamma-1}}+\frac{dy}{dx}u(1-W^2)^{\frac{1}{\gamma-1}}\\&\quad-\frac{2yuW}{\gamma-1}(1-W^2)^{\frac{-\gamma+2}{\gamma-1}}W_x\end{aligned}\right\}\tag{22}$$

When equations (21) and (22) are substituted in equations (15) and (17) and (16) and (18) and the Mach angle and the velocity are expressed in polar coordinates, equations (15) and (17) become

$$\frac{dy}{dx}=\tan(\beta+\varphi)\qquad\text{(first family)}\tag{23}$$

$$\frac{dy}{dx}=\tan(\varphi-\beta)\qquad\text{(second family)}\tag{24}$$

and equations (16) and (18) become

$$\frac{dW}{W}-\tan\beta\,d\varphi-\frac{dx}{y}l+\frac{dx}{dn}\frac{ds}{\gamma R}\frac{\sin^3\beta}{\cos(\beta+\varphi)}=0\ \text{(first family)}\tag{25}$$

$$\frac{dW}{W}+\tan\beta\,d\varphi-\frac{dx}{y}m-\frac{dx}{dn}\frac{ds}{\gamma R}\frac{\sin^3\beta}{\cos(\varphi-\beta)}=0\ \text{(second family)}\tag{26}$$

Equations (23) and (24) are identical to equations for potential flow (2) and (3), and equations (25) and (26) are similar to equations for potential flow (4) and (5), differing only by the terms that contain ds. Equations (23) to (26) permit a step-by-step calculation of the entropy, intensity of velocity, and direction of the velocity if the initial and boundary conditions are known. If all physical properties are known for two points A and B and if the two points are close to each other, the tangents to the characteristic lines at the points A and B can be substituted for the characteristic lines with close approximation. In this way a point C can be determined as the intersection of the second characteristic line of point B with the first characteristic line of point A (fig. 1), because φ and β are known for the points A and B.

For the characteristic lines of the first family, equation (25) gives the variation of φ and W from point A to point C, and all the coefficients are known and correspond to the coefficients for point A; only the term $\frac{ds}{dn}$ is unknown. From equation (26) the variation of φ and W from point B to point C can be determined, and all other terms, except $\frac{ds}{dn}$, are known and equal to the values for point B. The term $\frac{ds}{dn}$ can be determined from the value of the entropy for points A and B.

From figure 1, in equation (25) the term $\frac{ds}{dn}$ can be written as

$$\frac{ds}{dn}=\frac{(s_C-s_A)\cos(\beta_A+\varphi_A)}{(x_C-x_A)\sin\beta_A}\tag{27}$$

and in equation (26) can be written as

$$\frac{ds}{dn}=\frac{(s_B-s_C)\cos(\varphi_B-\beta_B)}{(x_C-x_B)\sin\beta_B}\tag{28}$$

If the points A and B are close to each other and the variation of entropy is gradual, equation (27) can be written as

$$\frac{ds}{dn}=\frac{s_B-s_A}{(x_C-x_A)\frac{\sin\beta_A}{\cos(\beta_A+\varphi_A)}+(x_C-x_B)\frac{\sin\beta_B}{\cos(\varphi_B-\beta_B)}}\tag{29}$$

and $\frac{ds}{dn}$ can be considered equal in equations (25) and (26). In this case $\frac{ds}{dn}$ is known; therefore φ and W can be calculated for point C. For practical calculations equations (25) and (26) should be transformed into two equations (equations (31) and (32)) each of which contains only one of the unknown terms dw and $d\varphi$.

For simplicity, let

$$\left.\begin{aligned}\xi_1&=x_A-x_B\\\xi_0&=x_C-x_A\\g&=1+\frac{\xi_1}{\xi_0}\\\Delta\varphi&=\varphi_A-\varphi_B\\h&=\frac{W_A}{W_B}\\e&=\frac{\sin\beta_A}{\cos(\beta_A+\varphi_A)}\\f&=\frac{\sin\beta_B}{\cos(\varphi_B-\beta_B)}\\r&=\tan\beta_B+h\tan\beta_A\\A&=\frac{s_B-s_A}{\gamma R}\frac{1}{e+gf}\end{aligned}\right\}\tag{30}$$

Then the following equations can be obtained:

$$r\,d\varphi_A=1-h-\Delta\varphi\tan\beta_B+A(gf\sin^2\beta_B+he\sin^2\beta_A)+\frac{\xi_0 m_B g}{y_B}-\frac{\xi_0 h l_A}{y_A}\tag{31}$$

$$\frac{dW_A}{W_A}=\tan\beta_A\,d\varphi_A-Ae\sin^2\beta_A+\frac{\xi_0 l_A}{y_A}\tag{32}$$

$$s_C=s_A+Ae\gamma R\tag{33}$$

$$\varphi_C=\varphi_A+d\varphi_A\tag{34}$$

$$W_C=W_A+dW_A\tag{35}$$

$$\sin^2\beta_C=\frac{\gamma-1}{2}\left(\frac{1}{W_C^2}-1\right)\tag{36}$$

In equation (31) the terms $\frac{\xi_0 m_B g}{y_B}$ and $\frac{\xi_0 h l_A}{y_A}$ become very important as y approaches zero, near the axis of the body; therefore, in this region the distance between the points considered must be reduced to obtain sufficient accuracy.

CHARACTERISTICS METHOD FOR TWO-DIMENSIONAL SUPERSONIC ROTATIONAL FLOW

In two-dimensional flow an equation similar to equation (13) can be obtained if a special stream function defined by the following equation is assumed (reference 8):

$$\left.\begin{aligned}\psi_y&=u(1-W^2)^{\frac{1}{\gamma-1}}\\ \psi_x&=-v(1-W^2)^{\frac{1}{\gamma-1}}\end{aligned}\right\} \qquad (37)$$

In this case the equation of motion (equation (13)) becomes (reference 8)

$$\left(1-\frac{u^2}{c^2}\right)\psi_{xx}-\frac{2uv}{c^2}\psi_{xy}+\left(1-\frac{v^2}{c^2}\right)\psi_{yy}$$
$$-(1-W^2)^{\frac{\gamma+1}{\gamma-1}}\left(\frac{W^2}{c^2}-1\right)f(\psi)=0 \qquad (38)$$

Equation (38), like equation (13), is a Monge-Ampère equation and permits the determination of two equations that define the characteristic lines and two equations that give the variation of the velocity along the characteristic lines. The equation with transformations analogous to the case of three-dimensional flow can be written in the following form:

$$\frac{dy}{dx}=\tan(\beta+\varphi) \quad \text{(first family)} \qquad (39)$$

$$\frac{dy}{dx}=\tan(\varphi-\beta) \quad \text{(second family)} \qquad (40)$$

$$\frac{dW}{W}-\tan\beta\,d\varphi+\frac{dx}{\gamma R}\frac{ds}{dn}\frac{\sin^3\beta}{\cos(\beta+\varphi)}=0 \quad \text{(first family)} \qquad (41)$$

$$\frac{dW}{W}+\tan\beta\,d\varphi-\frac{dx}{\gamma R}\frac{ds}{dn}\frac{\sin^3\beta}{\cos(\varphi-\beta)}=0 \quad \text{(second family)} \qquad (42)$$

Equations for φ and dW similar to equations (31) and (32) can be obtained from equations (39) to (42) by using equation (29) for the expression $\frac{ds}{dn}$ as follows:

$$r\,d\varphi_A=1-h-\Delta\varphi\tan\beta_B+A(gf\sin^2\beta_B+he\sin^2\beta_A) \qquad (43)$$

$$\frac{dW_A}{W_A}=\tan\beta_A\,d\varphi-Ae\sin^2\beta_A \qquad (44)$$

$$s_C=s_A+Ae\gamma R \qquad (45)$$

$$\varphi_C=\varphi_A+d\varphi_A \qquad (46)$$

$$W_C=W_A+dW_A \qquad (47)$$

$$\sin^2\beta_C=\frac{\gamma-1}{2}\left(\frac{1}{W_C^2}-1\right) \qquad (48)$$

DETERMINATION OF SHAPE OF SHOCK AND PRESSURE DISTRIBUTION ALONG A BODY

The physical properties of supersonic flow past a body of revolution in axially symmetrical flow can be determined step by step by the use of equations (31) to (36). The system of calculation is similar to that for potential flow. If the body begins with a point (reference 5), a cone tangent to the body (fig. 2) can be substituted for the front part of the body. If point A is the point at which the body can no longer be considered coincident with the cone, the velocity at point A is known from the cone calculations (references 9 and 10); therefore, the shape of the characteristic line AB of the first family can be designed, because φ and β corresponding to different angles θ are known from the cone calculations. At point A the body turns through an angle $\Delta\varphi$ and the flow undergoes a transformation that is determinable by the laws of two-dimensional flow. The velocity and direction of the flow after the deviation $\Delta\varphi$, therefore, and the tangents to the new characteristic lines of the first family at point A can be designed. At a point B, near point A, the intensity and direction of the velocity are known; consequently, the tangent to the characteristic line of the second family can be designed at point B, and the point C_1 can be located. At point C_1 the physical properties can be calculated with the equations of potential flow (equations (8) and (9)) because the shock in front of the body is conical. With the same system the point C_n is determined from the point B_n on the shock wave. In order to determine the flow of the point C_{n+1} on the shock wave, the equation across the shock and the equation for the characteristic lines of the first family must be used. If ϵ is the angle between the tangent to the shock and the direction of velocity of flow in front of the shock, δ the deviation of the direction of velocity across the shock wave, and the subscripts a and b denote the conditions ahead of and behind the shock, respectively, the shock equations can be written in the following form (reference 11):

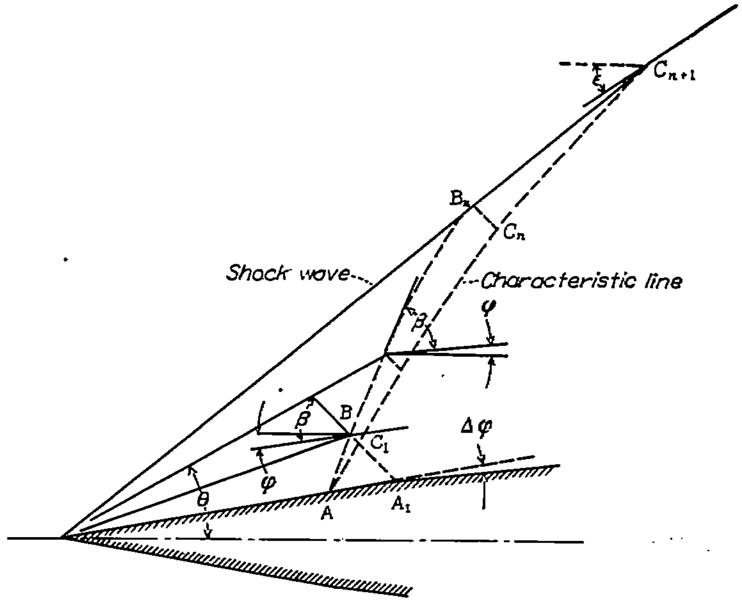

FIGURE 2.—Practical system of calculating the flow field for a pointed-nose body of revolution.

$$\frac{\tan\epsilon}{\tan(\epsilon-\delta)}=\frac{2}{\gamma+1}\left[\frac{1}{M_b^2\sin^2(\epsilon-\delta)}+\frac{\gamma-1}{2}\right] \qquad (49)$$

$$\frac{1}{\tan\delta}=\left(\frac{\gamma+1}{2}\frac{M_a^2}{M_a^2\sin^2\epsilon-1}-1\right)\tan\epsilon \qquad (50)$$

$$\frac{p_b}{p_a}=\frac{2\gamma}{\gamma+1}\left(M_a^2 \sin^2 \epsilon-\frac{\gamma-1}{2\gamma}\right) \tag{51}$$

$$\frac{\rho_a}{\rho_b}=\frac{2}{\gamma+1}\left(\frac{1}{M_a^2 \sin^2 \epsilon}+\frac{\gamma-1}{2}\right) \tag{52}$$

$$s_b-s_a=\frac{R}{\gamma-1}\left(\log_e \frac{p_b}{p_a}+\gamma \log_e \frac{\rho_a}{\rho_b}\right) \tag{53}$$

$$\frac{1}{W^2}=1+\frac{2}{\gamma-1}\frac{1}{M_b^2} \tag{54}$$

Equations (51) to (53) show that the general condition for obtaining potential flow behind the shock when the flow in front of the shock is potential is that $M_a \sin \epsilon$ must be constant. Since the value of M_a in front of the shock is known from equations (49) to (54), the values of $\frac{d(s_b-s_a)}{d\delta}$ and $\frac{dW}{d\delta}$ can be determined as functions of δ and therefore the equation for the characteristic lines of the first family (equation (25)) becomes

$$\frac{W_{\varphi_{C_n}}-W_{C_n}}{W_{C_n}}+\frac{dW}{d\delta}\frac{d\varphi}{W_{C_n}}-\tan \beta_{C_n}\, d\varphi-\frac{dx}{y_{C_n}}\, l_{C_n}$$
$$+\frac{\sin^2 \beta_{C_n}}{\gamma R}\left[s_{\varphi_{C_n}}-s_{C_n}+\frac{d(s_b-s_a)}{d\delta}\, d\varphi\right]=0 \tag{55}$$

where $W_{\varphi_{C_n}}$ is the velocity behind the shock, $s_{\varphi_{C_n}}$ is the entropy, $\frac{dW}{d\delta}$ and $\frac{d(s_b-s_a)}{d\delta}$ are coefficients that correspond to a deviation across the shock for which the velocity assumes the direction of φ_{C_n}, W_{C_n} is the velocity, and s_{C_n} is the entropy at the point C_n. When the value of $d\varphi$ has been determined, the deviation across the shock δ and the corresponding values of W and ϵ can be determined at point C_{n+1}.

In order to determine the velocity on the body at a point A_1, equation (26) is used. At point A_1 the value of φ is known because the direction of the flow is tangent to the body and, therefore, $d\varphi$ is known; $\frac{ds}{dn}$ is also known because in equation (27) the value of s_C corresponds to the value of s at the point A_1 and is equal to the value at point A, which is known from the cone calculation. From the value of W, the pressure on the body relative to the pressure p_0' (pressure for zero velocity from isentropic transformation from the conditions behind the shock) can be determined as

$$\frac{p}{p_0'}=(1-W^2)^{\frac{\gamma}{\gamma-1}} \tag{56}$$

On the lip of the nose of an open-nose body a shock wave that is a two-dimensional shock occurs; therefore, the tangent to the shock on the lip is known and the pressure and velocity behind the shock are also known (equations (49) to (54)). In figure 3 the line AB and the velocity behind the shock at point B are known. With equation (26) the velocity at point C can be calculated with the system just described, and from the point B the point D along the characteristic line of the first family can be calculated by equation (55). From point D the point E can be calculated and a point F can be interpolated, which permits the determination of points G and H. Because the curvature of the shock near the lip is large, a point C that is very near point A must be selected so that correct interpolated values may be obtained. The point E can be recalculated from point G, and the points I and M can be recalculated from point F in order to have a second approximation.

For the case of two-dimensional flow the procedure is the same as that for three-dimensional flow; equations (43) to (48) are used instead of the corresponding equations (equations (31) to (36)).

EXAMPLES OF APPLICATION OF CHARACTERISTICS METHOD FOR ROTATIONAL FLOW

DETERMINATION OF SHOCK SHAPE AND PRESSURE DISTRIBUTION ALONG THE EXTERNAL SURFACE OF A SLENDER OPEN-NOSE BODY OF REVOLUTION

Theoretical and experimental calculations were made to determine the shock shape and pressure distribution along the external surface of a slender open-nose body of revolution. The body considered is the same body for which calculations of the external pressure distribution were made by Brown and Parker of the Langley Memorial Aeronautical Laboratory by use of the small-disturbance theory. The calculations were made for a free-stream Mach number of 1.525, for which a schlieren photograph taken during tests was available for comparison of the calculated and test results.

In order to determine the importance of rotation of the flow, calculations for the front part of the body were also made with the potential-flow characteristic equations. The results of these calculations differed only slightly from those obtained from the characteristics method for rotational flow because the curvature of the shock was very small. The

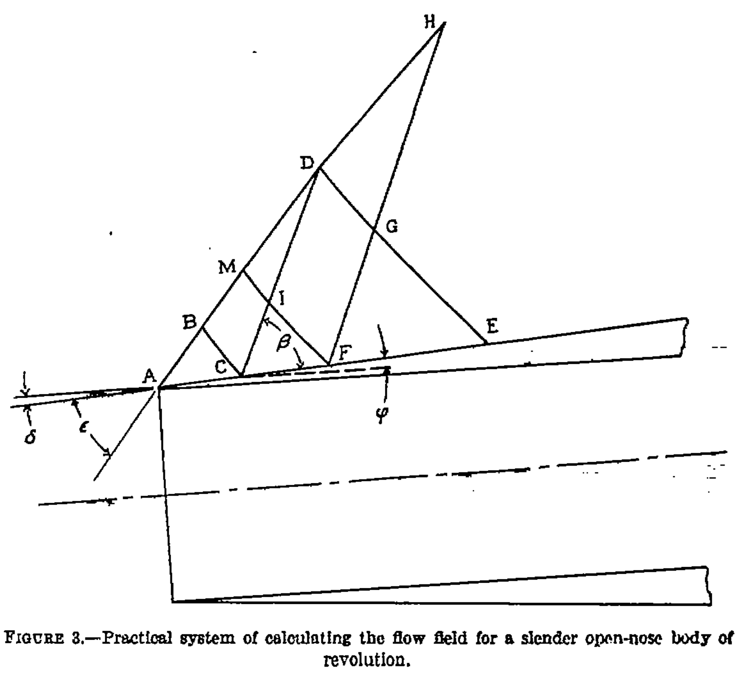

FIGURE 3.—Practical system of calculating the flow field for a slender open-nose body of revolution.

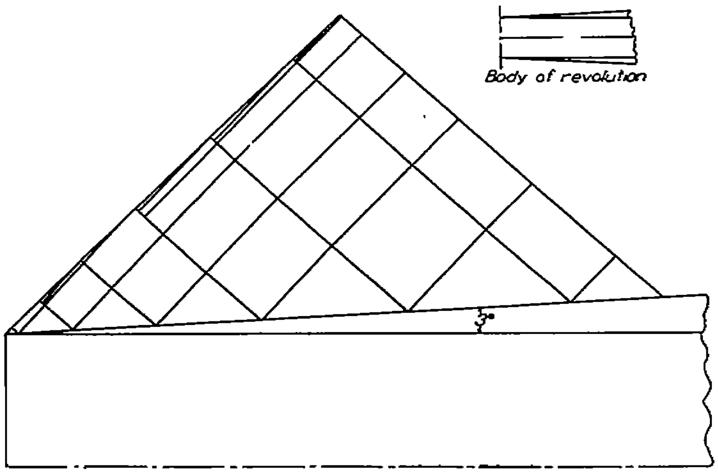

FIGURE 4.—Practical system of calculating the external flow around a slender open-nose body of revolution for $M=1.525$.

calculations were begun with the determination of the two-dimensional shock on the lip of the nose. The practical system of the calculations is shown in figure 4, and in figure 5 the calculated streamlines and shock-wave shape are compared with the shock-wave shape obtained from test results. In figure 6 the pressure distribution calculated by the characteristics method is compared with the pressure distribution determined by the small-disturbance theory. The small-disturbance theory undervalues the increase in pressure that occurs through the shock, but the differences in the results obtained by this method and those obtained by the characteristics method are small.

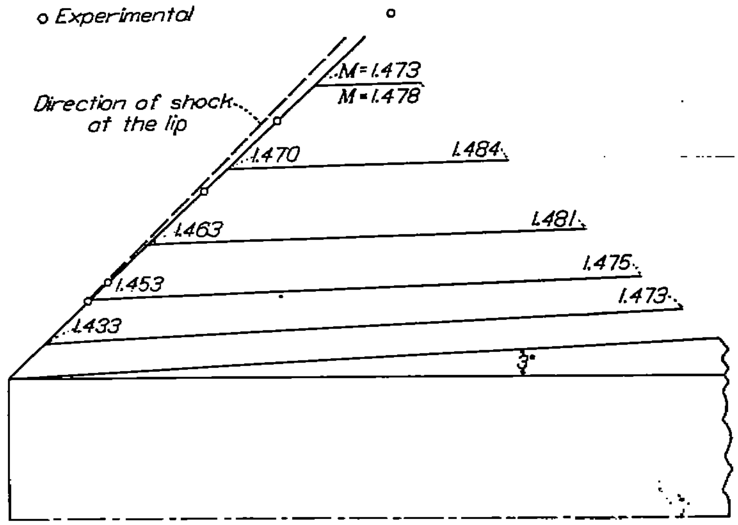

FIGURE 5.—Calculated streamlines and shock wave for a slender open-nose body of revolution for $M=1.525$, showing experimental shock-wave shape.

DETERMINATION OF SHOCK SHAPE, STREAMLINES, AND PRESSURE DISTRIBUTION ALONG THE INTERNAL SURFACE OF A SLENDER OPEN-NOSE BODY OF REVOLUTION

Three slender open-nose bodies with different conical inlet angles are considered (figs. 7 to 12) and the supersonic part of the internal flow is studied for a free-stream Mach number of 1.6. For this type of body the internal shock produced at the lip of the inlet has a very large curvature and the effect of rotation is therefore very important. The calculations are extended to the region in which the Mach number is 1.0.

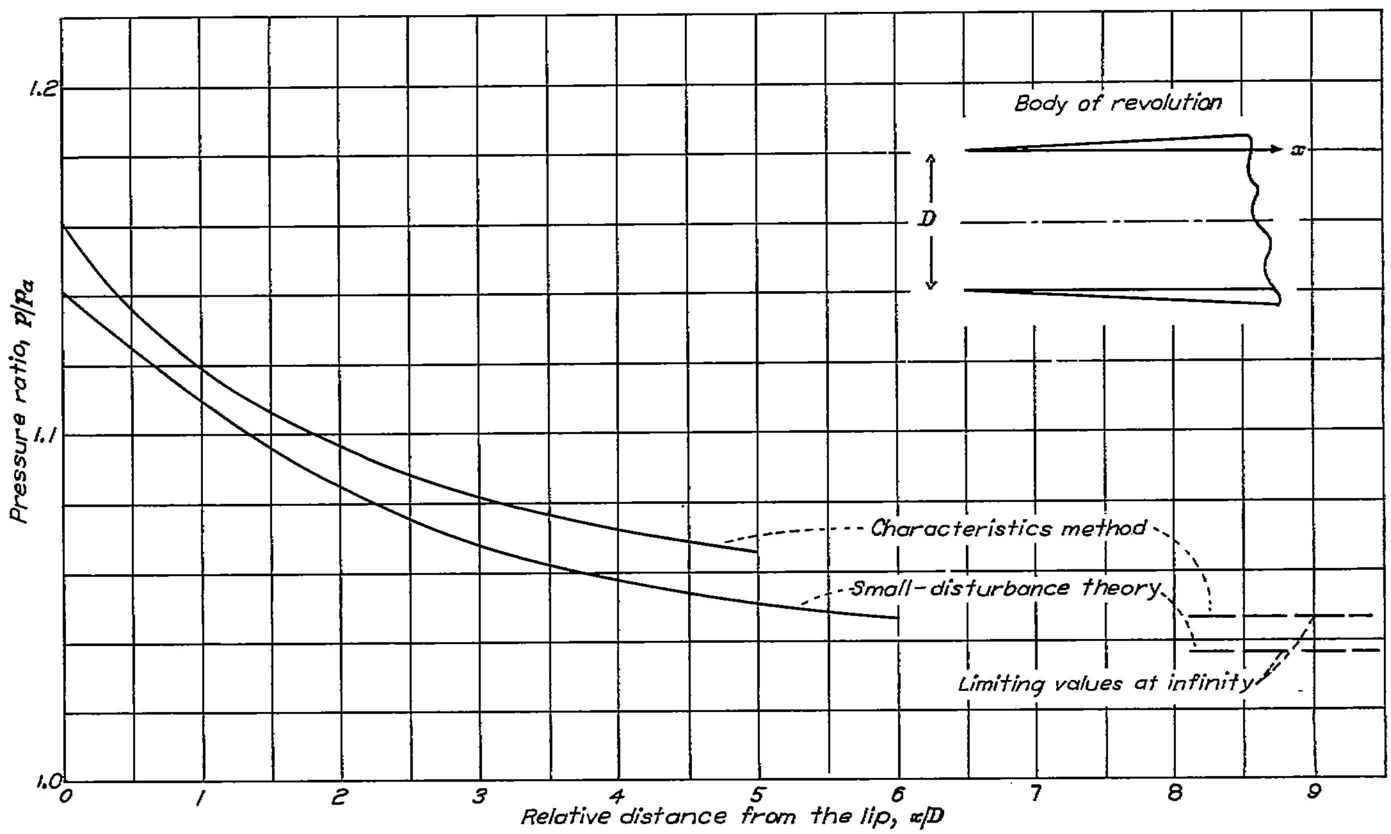

FIGURE 6.—Pressure distribution along the external surface of a slender open-nose body of revolution for $M=1.525$. (Data for small-disturbance theory from work by Brown and Parker of the Langley Laboratory.)

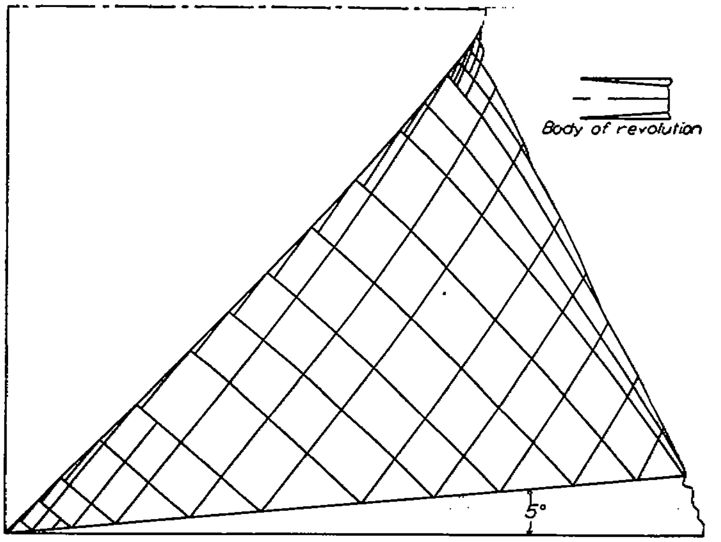

FIGURE 7.—Practical system of calculating the internal supersonic-flow quantities for a slender open-nose body of revolution for $M=1.6$.

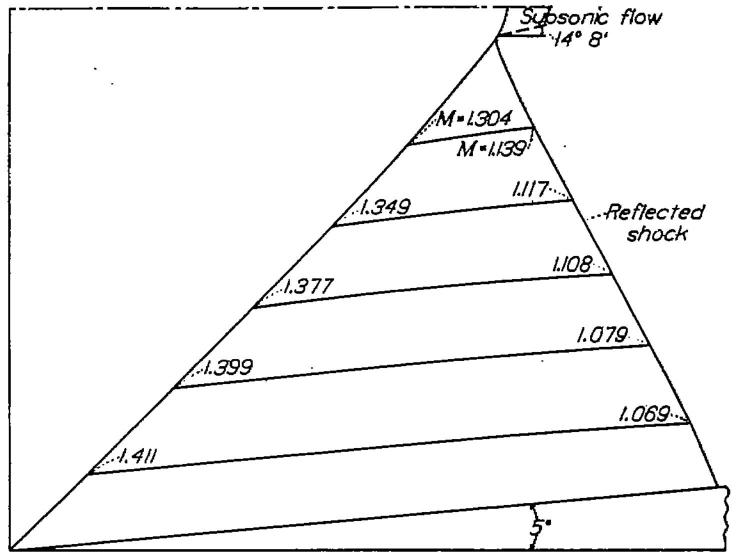

FIGURE 8.—Calculated streamlines and shock wave for internal flow in a slender open-nose body of revolution for $M=1.6$.

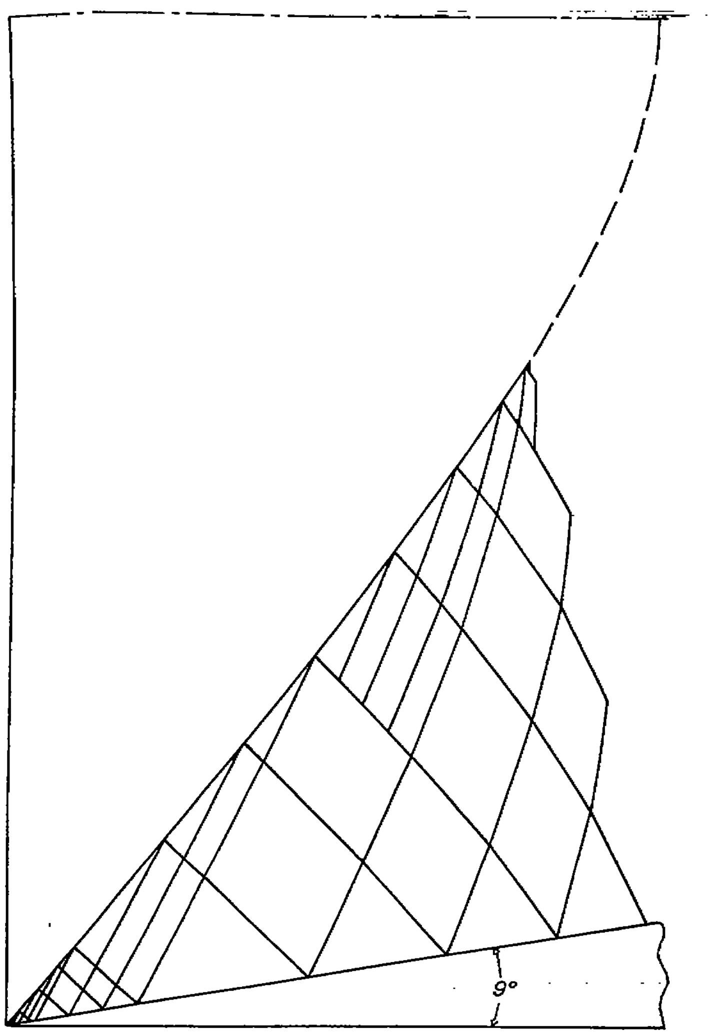

FIGURE 9.—Practical system of calculating the internal-supersonic-flow properties for a slender open-nose body of revolution for $M=1.6$.

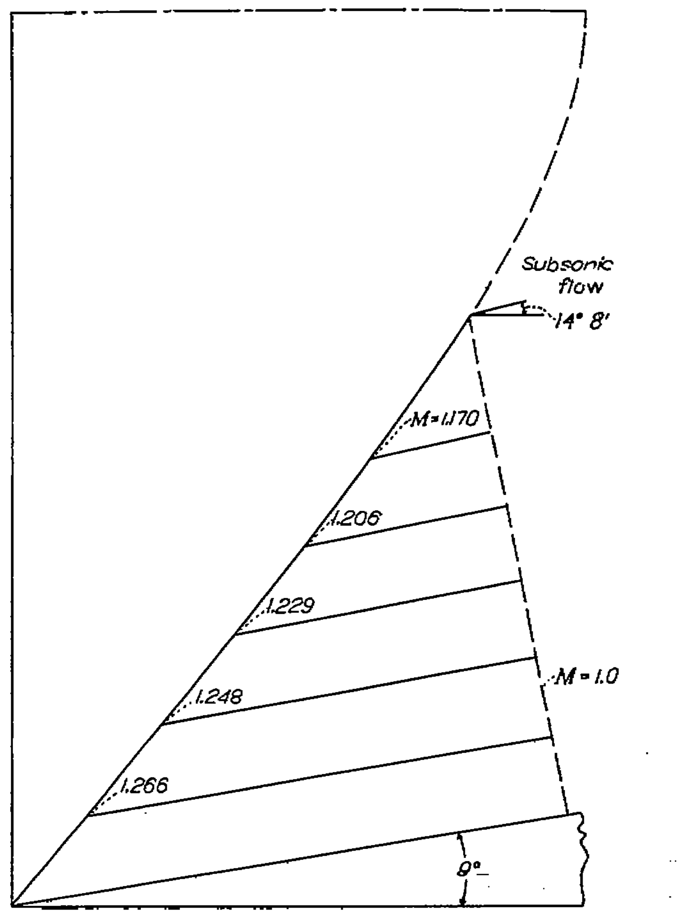

FIGURE 10.—Calculated streamlines and shock wave for internal flow in a slender open-nose body of revolution for $M=1.6$.

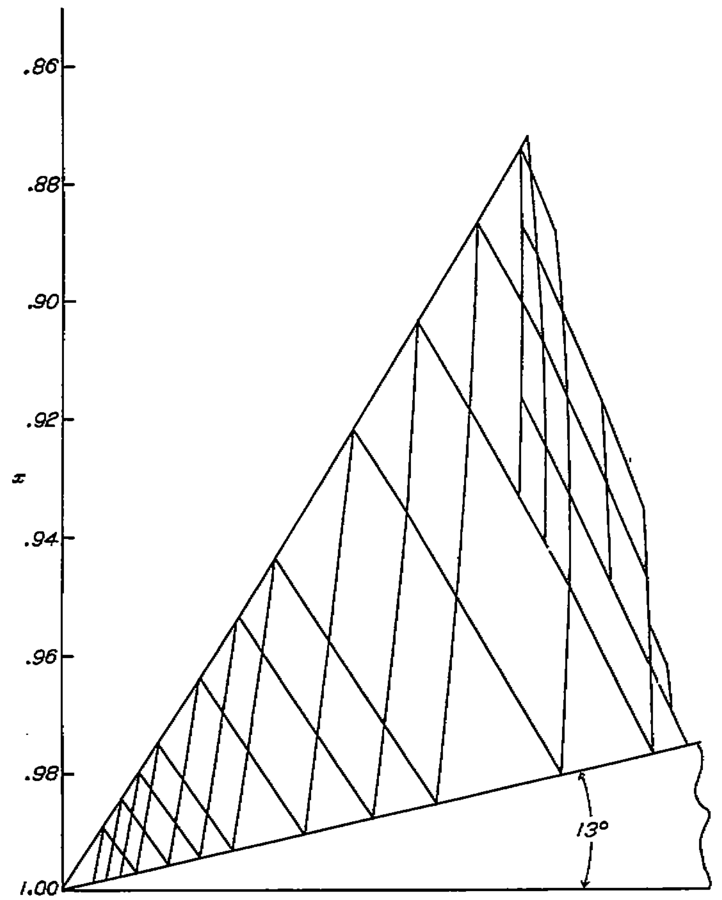

FIGURE 11.—Practical system of calculating the internal supersonic-flow properties for a slender open-nose body of revolution for $M=1.6$.

The hypothesis is made that subsonic boundary conditions and stability considerations permit a subsonic flow at the end of the supersonic flow such as results from the calculations. The results of the calculations show that at the axis of the inlet a normal shock always occurs and that the region in which a strong shock occurs (with subsonic velocity behind the shock) increases in extension with the increase in angle of the internal cone. When the cone angle approaches zero and the shock is a Mach wave, a complete reflection occurs at the axis of the inlet and the extension of the strong shock is zero.

For large internal cone angles (figs. 9 to 12) the shock is a simple shock that becomes normal in the central part of the body of revolution. After the shock the compression continues but the characteristic lines cannot form an envelope. For small internal cone angles compression occurs gradually and an envelope of Mach lines occurs. The shock therefore reflects from the central part and another shock is generated. The form of the reflected shock is shown in figure 8. The ratio of the diameter of the region in which a strong shock occurs to the diameter of the inlet as a function of the internal cone angle is shown for $M=1.6$ in figure 13. The results are interesting for the practical design of supersonic inlets of slender shape because they show that for large cone angles the central part of the body of revolution, in which the compression is not very efficient, is large.

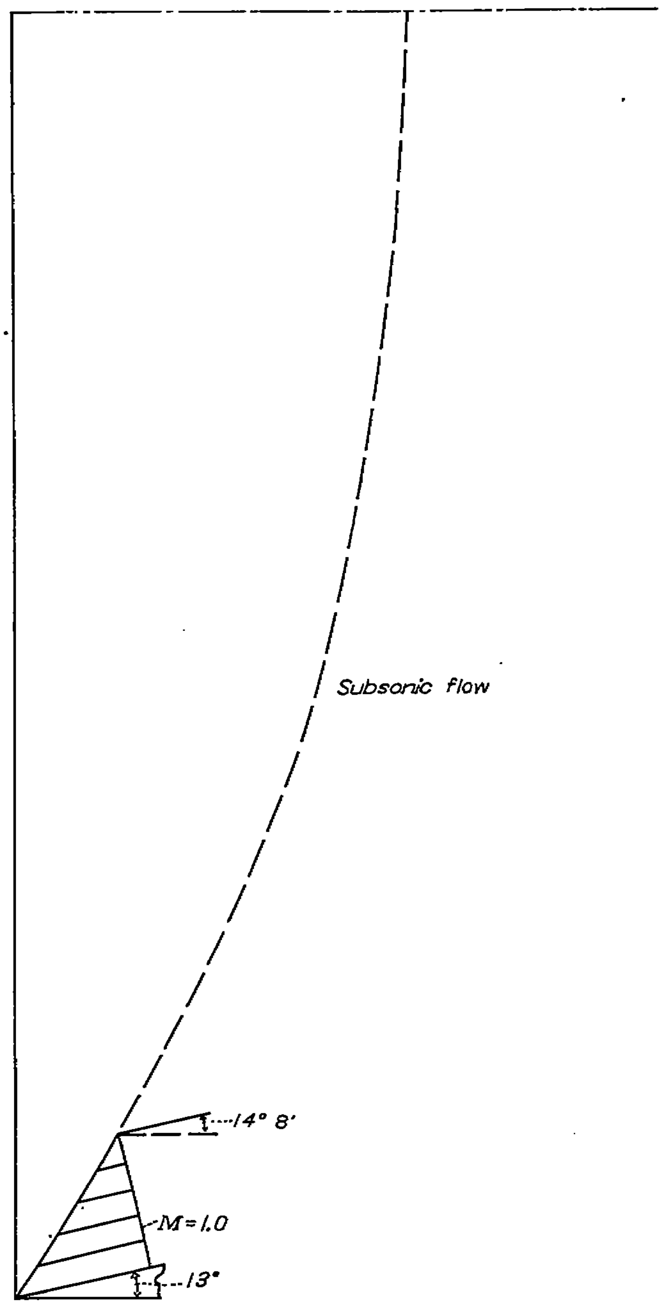

FIGURE 12.—Calculated streamlines and shock wave for internal flow in a slender open-nose body of revolution for $M=1.6$.

DETERMINATION OF PHYSICAL PROPERTIES OF THE INTERNAL FLOW THROUGH AN INLET WITH A CENTRAL BODY

For a Mach number of 1.6 an analysis of the shape of an inlet with a central body was made to aid in obtaining high efficiency. Theoretically a supersonic diffuser with or without a central body and having no shock losses or shock drag can be obtained (reference 12); but for practical use it is convenient to accept small shock drag in order to avoid large friction drag. The inlet considered (fig. 14) has a 10° central cone. The deviation across the conical shock is 48′. The shock is reflected by a cylinder that forms the external part of the inlet. The reflected shock produces rotational flow behind the shock and the deviation across this shock on the

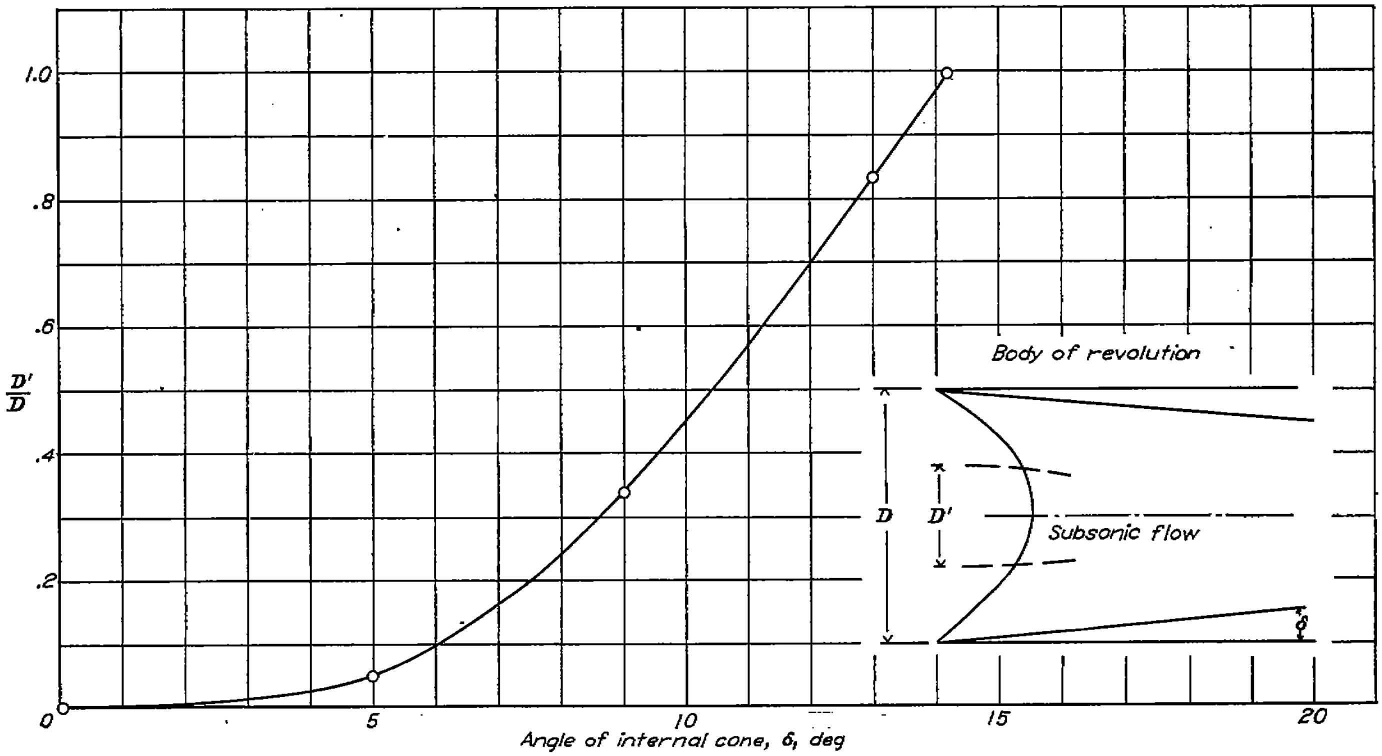

FIGURE 13.—Ratio of the diameter of the region in which strong shock occurs to the diameter of the inlet as a function of the angle of internal cone. $M=1.6$.

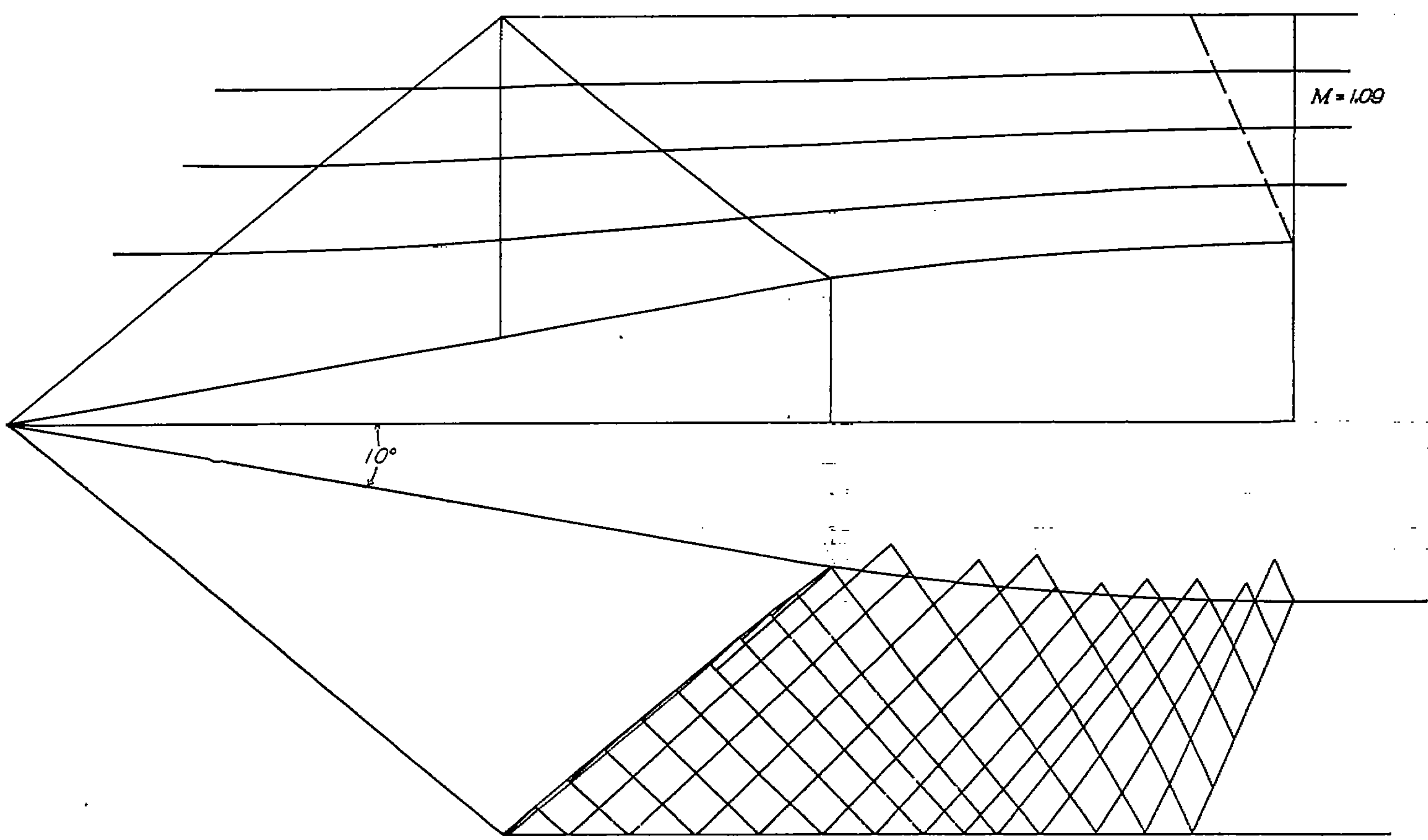

FIGURE 14.—Practical system of calculating the shape of the central body, of the streamlines, and of shock-wave shape for a supersonic inlet at $M=1.6$.

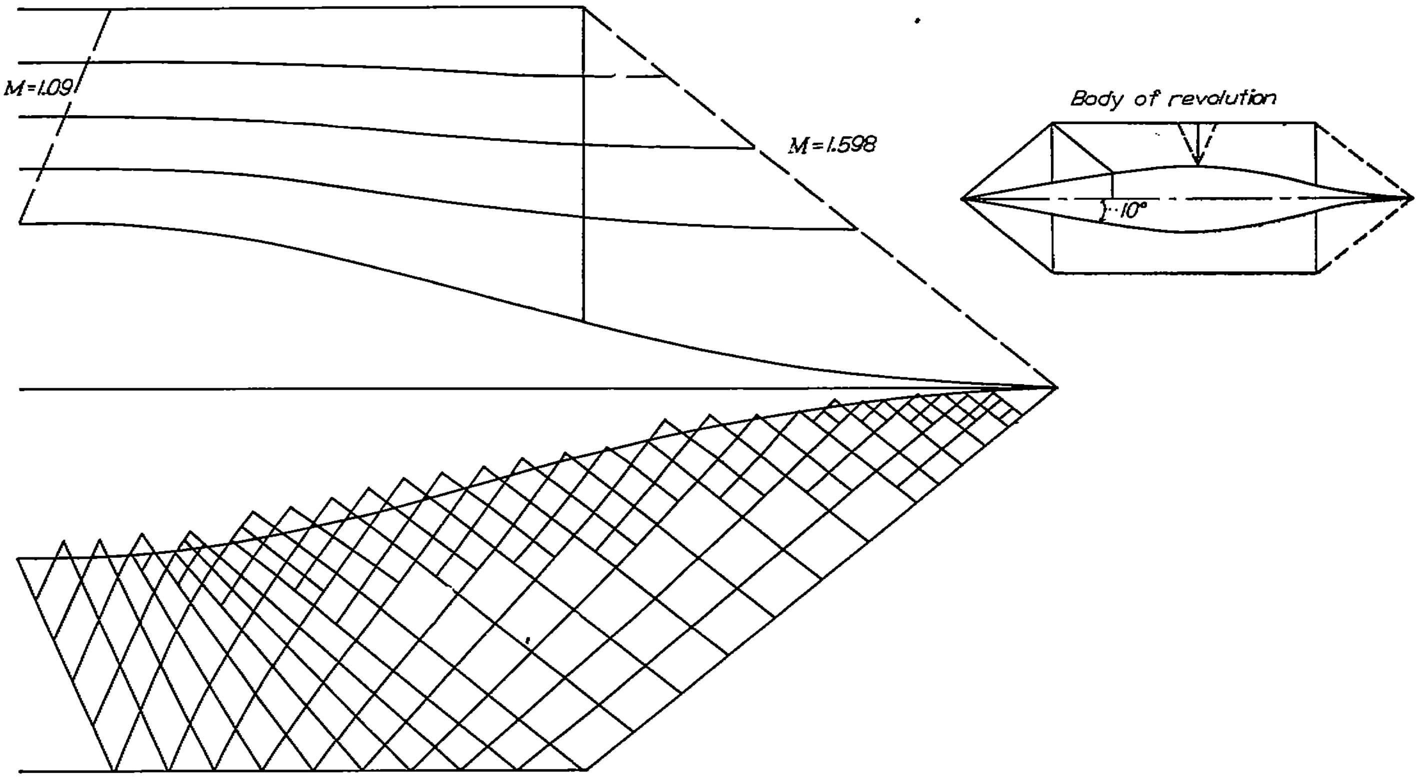

FIGURE 15.—Practical system of calculating the shape of the central body and of the streamlines of the tail of a body without pressure drag for $M=1.6$.

cylinder is 1° and on the central body, 2° 43′. If the central body behind the shock has the same direction as the velocity, the shock will not be reflected and isentropic compression can be obtained behind the shock (fig. 14). The design of the central body, therefore, was determined from the calculation of the corresponding streamline. The variation of the velocity along the external cylinder and the value of the exit velocity were fixed, and from this condition and the condition dependent on the shock, the velocity at every point was calculated. In order to avoid errors stream tubes were designed that permitted, on the basis of the ratio of the area in the region of uniform velocity to the area at the end of the stream tube, a check on the precision of the numerical calculations. The Mach number in the minimum section of the inlet was fixed at a value larger than 1.0 so that disturbances from the subsonic part of the flow would not cause instability. The value chosen was 1.09.

If an effuser is connected with the diffuser, a body of revolution with very low shock drag can be obtained (fig. 15). The only pressure losses are the losses across the two shocks, which are very small; but for practical applications the friction losses are larger than for the internal body alone. A balance of the pressure losses and friction losses must therefore be made in order to examine the possibility of practical use of this arrangement.

CONCLUSIONS

A system for calculating the physical properties of supersonic rotational flow with axial symmetry and supersonic rotational flow in a two-dimensional field was determined by use of the characteristics method. Practical use of the system is based on a step-by-step procedure, which requires long numerical calculations; but the calculations for three-dimensional flow are of the same type as for potential flow and, therefore, can be used for the practical problems in which rotation is important. Some applications were made to determine the external and internal flow on bodies of revolution with axial symmetry, and the following conclusions were indicated:

1. The effect of rotation is not very important if the variation of entropy is small but is important in the study of internal flow, for which the variation of entropy is usually large.
2. When the inlet is a circular conical channel, a shock is produced at the lip of the inlet that becomes stronger when the shock approaches the axis of the inlet and becomes a normal shock at the axis. The region in which a strong shock occurs (with subsonic velocity behind the shock) increases with the increase of the angle of internal cone.
3. If an inlet with a central body is considered, the method of characteristics permits the design of an internal-channel shape that, theoretically, results in very efficient recompression in the inlet; and, if an effuser is connected with the diffuser, a body of revolution with very small shock-wave drag can be determined.

LANGLEY MEMORIAL AERONAUTICAL LABORATORY,
NATIONAL ADVISORY COMMITTEE FOR AERONAUTICS,
LANGLEY FIELD, VA., *April 29, 1946.*

REFERENCES

1. Prandtl, L., and Busemann, A.: Näherungsverfahren zur zeichnerischen Ermittlung von ebenen Strömungen mit Überschallgeschwindigkeit. Stodola Festschrift, Zürich and Leipzig, 1929.
2. Busemann, A.: Gasdynamik. Handb. d. Experimentalphys., Bd. IV, 1. Teil, Akad. Verlagsgesellschaft m. b. H. (Leipzig), 1931, pp. 343–460.
3. Frankl, F. I.: Supersonic Flows with Axial Symmetry. Izvestia Akademii RKKA, vol. I, 1934.
4. Ferrari, C.: Campo aerodinamico a velocità iperacustica attorno a un solido di rivoluzione a prora acuminata. L'Aerotecnica, vol. XVI, fasc. 2, Feb. 1936, pp. 121–130.
5. Ferrari, C.: The Determination of the Projectile of Minimum Wave-Resistance. R.T.P. Translation No. 1180, British Ministry of Aircraft Production. (Part II from Atti R. Accad. Sci. Torino, vol. 75, Nov.-Dec. 1939, pp. 61–96.)
6. Guderley, G.: Die Charakteristikenmethode für ebene und achsensymmetrische Überschallströmungen. Jahrb. 1940 der deutschen Luftfahrtforschung, R. Oldenbourg (Munich), pp. I 522 – I 535.
7. Sauer, R.: Charakteristikenverfahren für räumliche achsensymmetrische Überschallströmungen. Forschungsbericht Nr. 1269, Deutsche Luftfahrtforschung (Aachen), 1940.
8. Crocco, L.: Una nuova funzione di corrente per lo studio del moto rotazionale dei gas. Rend. della R. Accad. dei Lincei. Vol. XXIII, ser. 6, fasc. 2, Feb. 1936.
9. Busemann, A.: Drücke auf kegelförmige Spitzen bei Bewegung mit Überschallgeschwindigkeit. Z.f.a.M.M., Bd. 9, Heft 6, Dec. 1929, pp. 496–498.
10. Taylor, G. I., and Maccoll, J. W.: The Air Pressure on a Cone Moving at High Speeds. Proc. Roy. Soc. (London), ser. A, vol. 139, no. 838, Feb. 1, 1933, pp. 278–311.
11. Crocco, Luigi: Singolarità della corrente gassosa iperacustica nell'intorno di una prora a diedro. L'Aerotecnica, vol. XVII, fasc. 6, June 1937, pp. 519–534.
12. Ferrari, C.: Campi di corrente ipersonora attorno a solidi di rivoluzione. L'Aerotecnica, vol. XVII, fasc. 6, June 1937, pp. 507–518.